Commputing&AI Connect
ISSN: 3104-4719
2025, Article ID. x, Cite as: https://www.doi.org/10.69709/xxx

SCIFINITI PUBLISHING

OPEN ACCESS

Research Article

6G Communication Systems Utilizing Intelligent Reflective Surfaces for Improved Data Rates Based on AI

Jehan Kadhim Shareef Al-Safi[1] Abbas Thajeel Rhaif Alsahlanee[2,*]

[1] Digital Media Department, Faculty of Media, University of Thi-Qar, Nasiriyah, Thi-Qar, Iraq; jihan.k.shareef@utq.edu.iq
[2] Faculty of Education for Humanities, University of Thi-Qar, Nasiriyah, Thi-Qar, Iraq; abbas.thajeel@utq.edu.iq

Abstract

Intelligent Reflecting Surfaces (IRS) are pivotal for energy-efficient 6G networks, yet optimizing their performance for simultaneous high data rates and energy efficiency remains a complex challenge. This paper leverages artificial intelligence (AI) to address this problem by introducing a novel AI-based optimization algorithm: Dynamic and Static Particle Swarm Optimization (DS-PSO). The proposed AI method intelligently learns the optimal phase-shift configuration for IRS elements, dynamically balancing exploration and exploitation to maximize the signal-to-noise ratio at the receiver. Simulation results demonstrate the efficacy of our AI-driven approach, showing our AI-optimized IRS model achieves a superior energy efficiency up to 269% higher than a standard IRS at a 10 bits/s/Hz data rate. This study underscores the significant potential of AI algorithms in mastering the intricate trade-offs of next-generation communication systems, positioning our model as a formidable solution for sustainable 6G connectivity.

Keywords:

artificial intelligence; energy efficiency; IRS-aided communication systems; meta surfaces; reconfigurable intelligent surface

1. Introduction

The intelligent reflecting surface (IRS) has emerged as a promising technique to address the challenges of sixth-generation (6G) wireless communication systems by enhancing propagation settings, therefore mitigating the effects of high route Line of Sight (LOS) [1]. An intelligent radio environment has recently developed to meet the stringent criteria for communication and sensing imposed by future 6G systems [2]. In this approach, the digitally-controlled metasurface, also known as a reconfigurable intelligent surface (RIS) or IRS, wirelessly alters the propagation environment to enhance wireless communication and radar sensing [3].

Metasurfaces are a novel type of functional material containing artificially periodic or quasiperiodic structures on sub-wavelength length scales [4,5]. IRS metasurface unit cells have active elements that allow electrical adjustment of electromagnetic waves, making them programmable [6,7]. Metasurfaces exhibit negative permittivity and permeability [8]. Metasurfaces may change electromagnetic waves from microwave to visible light. The quality of wireless communications might change over time due to the unpredictable nature of radio propagation. During the propagation of electromagnetic waves, free-space route line-of-sights (LOSs), reflections, refractions, signal absorption, and diffractions induced by physical objects make wireless channels very dynamic [9] IRS's capacity to

* Corresponding Author:
Abbas Thajeel Rhaif Alsahlanee, Faculty of Education for Humanities, University of Thi-Qar, Nasiriyah, Thi-Qar, Iraq, abbas.thajeel@utq.edu.iq; Tel.: +xx-xxx-xxx-xxxx

manipulate electromagnetic waves in real-time gives up endless possibilities to change the design paradigm of wireless communications from "adapting to wireless channels" toward "changing wireless channels" [9,10]. In particular, IRS can achieve desirable functions by dynamically regulating phase shifts using low-cost reflecting elements, including multi-antenna/MIMO (multiple-input multiple-output) channel rank improvement, environment obstacle avoidance, and reshaping channel realizations/distributions [11].

Improved communication system performance is possible when transmit beamforming is used with an IRS that uses a phase-shift design [12,13]. Transmit beamforming can also synthesize multiple beams toward existing users and targets [12–14].

The creation of the IRS reflection pattern (passive beamforming) requires channel state information (CSI) of the sub-channels between wireless transceivers and IRS [15]. IRS cannot detect the incident signal because it is passive, making the estimation process more complex than other wireless communication systems [16]. Moreover, previous studies have expanded the scope of the analysis to include general channel models, such as fading, in addition to practical defects such as transceiver misalignment, phase errors, and mobile interference [17,18]. In contrast, by dynamically optimizing the phase, the IRS may strengthen the signal of the communications system [19].

Multiple performance metrics, such as spectral efficiency (SE), transmit power, sum rate, throughput, security, and others, have been the focus of substantial research into the use of IRS in wireless communication [20]. In addition, the literature discussed the energy efficiency (EE) metric as a means of assessing the performance of IRS within wireless communication networks, as in [2,10,20].

We have performed multiple studies on the application of AI-driven optimisation techniques to enhance Recommender Systems, communications, and networks, including: [21–26].

This paper aims to enhance the energy efficiency of an IRS system for optimizing transmission performance in 6G communication systems while guaranteeing high data rates. Artificial intelligence (AI) techniques can be utilized to reprogram the IRS system, resulting in improved performance of the newly developed models. An AI algorithm called DS-PSO (dynamic and static with particle swarm optimization) has been proposed to enhance the standard IRS model's performance. The IRS system can support the highest energy efficiency with the highest data rates. Accordingly, the selection between standard IRS and optimized IRS (IRS^o) models impact energy efficiency and data rates. An IRS's energy efficiency depends on data rates. The proposed optimization algorithm enhances energy efficiency and data rates. However, the data rates determine the necessary enhanced energy efficiency for the (IRS^o) model. Thus, the mathematical equations formulated in this proposed paper are used to determine the energy efficiency and data rates of an (IRS^o) model.

While the existing literature provides a strong foundation for IRS-assisted communication, several research gaps remain unaddressed, which this work aims to fill. Firstly, many studies focus on optimizing for spectral efficiency or throughput but lack a comprehensive analysis of the critical trade-off between energy efficiency (EE) and high data rates in multi-IRS 6G scenarios. Secondly, while algorithms like standard PSO and GA have been applied, they often suffer from premature convergence to local optima for the complex, high-dimensional problem of IRS phase-shift optimization, indicating a need for more robust hybrid optimization techniques. Finally, there is a lack of systematic comparison under a unified framework that benchmarks proposed models against standard IRS, SISO, and a range of existing works (e.g., single, double, triple IRS, PSO-IRS, GA-IRS) using the practical metric of EE versus data rate. This paper seeks to address these limitations by proposing a novel AI-driven hybrid algorithm and a rigorous comparative performance analysis.

We address these limitations by proposing a novel AI-driven hybrid algorithm and conducting a rigorous comparative performance analysis.

The primary innovations of this paper are as follows: (1) We propose a novel hybrid Dynamic and Static Particle Swarm Optimization (DS-PSO) algorithm, specifically designed to overcome the limitations of traditional optimizers for the complex, non-convex problem of IRS phase-shift optimization. Its hybrid topology provides a superior balance between exploration and exploitation. (2) We develop a comprehensive analytical framework for an IRS^o model, deriving the key performance metrics for energy efficiency and data rate. (3) We conduct an extensive simulation study benchmarking the proposed model against a standard IRS, a SISO baseline, and state-of-the-art works from the literature (including PSO-IRS, GA-IRS, and multi-IRS configurations). (4) We demonstrate that our (AI-IRS^o) model achieves superior performance, specifically up to 269\% higher energy efficiency than a standard IRS at high data rates, providing a critical solution for 6G networks.

The remainder of this paper is organized as follows: Section 2 describes the system model, analytical performance framework, and the proposed AI optimization method. Section 3 presents simulation results and performance comparisons. Section 4 discusses practical implementation challenges. Finally, Section 5 will outline the conclusion and future work.

2. Methods

This section outlines the system model, analytical performance framework, and the proposed AI optimization algorithm used to evaluate the enhanced IRS-aided 6G communication system.

2.1. System Model

Here, we focus on one-to-one transmissions, where the source and destination each have a single antenna, where $h_{sd} \in \mathbb{C}$ represents the deterministic flat-fading channel, while the destination receives a signal as in (1).

$$y = h_{sd}\sqrt{p}s + n \tag{1}$$

where $n \sim \mathcal{N}c(0, \sigma^2)$, denotes the noise at the receiver, s stands for the unit-power information signal, and p is the transmit power. This notation makes antenna gains easy to see by including them in the channels. Equation (2) describes the capacity of this SISO channel, which is (single-input-single-output).

$$R_{\text{SISO}} = log_2\left(1 + \frac{p|h_{sd}|^2}{\sigma^2}\right) \tag{2}$$

A higher transmission capacity during wireless communication can be achieved by using additional technologies. The IRS can be one of the technologies that enhances the data transmission capacity of wireless communication systems. IRSs can outperform relays at processing deterministic flat-fading channels, channel estimation, and frequency-selective fading. In terms of performance, deterministic flat-fading channels achieve the best performance [27].

It is important to note that while our analysis and simulations assume deterministic flat-fading channels for clarity and mathematical tractability, frequency-selective fading is indeed prevalent in real-world environments. In such scenarios, the performance comparison between IRS and relays becomes more complex.

A key advantage of relays is their ability to perform active processing, including amplification and equalization, which can mitigate inter-symbol interference caused by frequency-selective fading. An IRS, being passive, cannot perform such active equalization. Its effectiveness in wideband systems depends on its ability to create a frequency-flat response or on employing more advanced, frequency-selective phase shift designs, which is an active area of research. Therefore, while the IRS holds a fundamental advantage in power efficiency and potential spatial gain over relays in flat-fading conditions, its deployment in strong frequency-selective environments requires careful consideration and may involve trade-offs compared to active relays; this presents a compelling direction for future work.

This paper examines the properties of the IRS. We enhance specific properties to achieve an optimized model of the IRS. Subsequently, we compare the standard and (IRS^o) models to ascertain their strengths and weaknesses. To conduct this study, we created a comprehensive transmission diagram in the wireless communication system using either the standard IRS or the proposed (IRS^o), as shown in Figure 1.

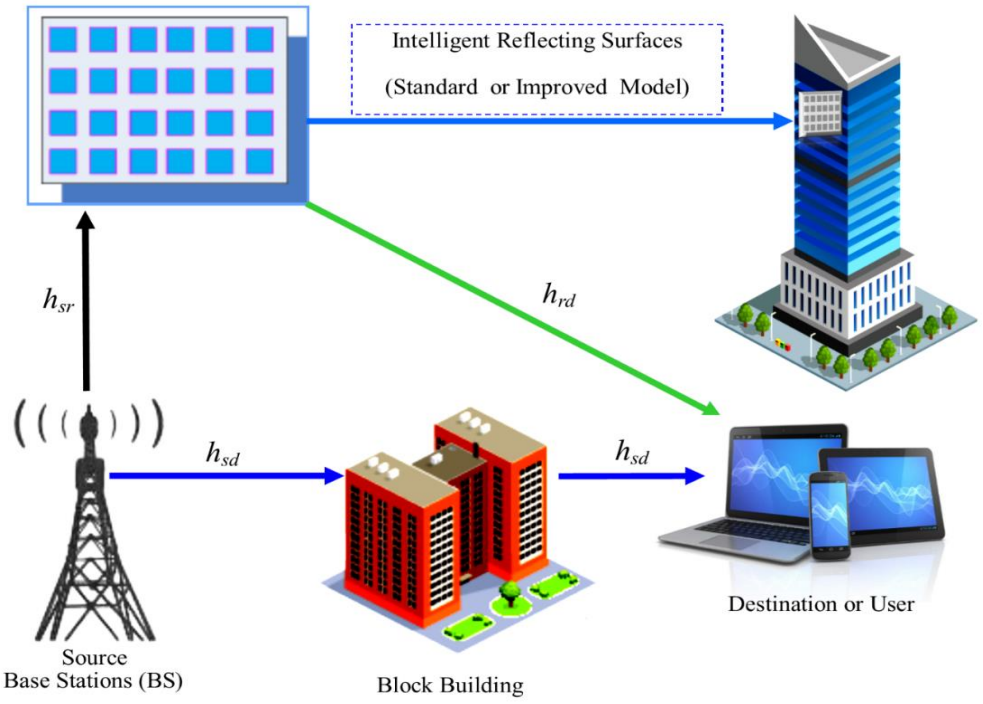

Figure 1. Standard IRS model/Improved IRS model aided transmission. *(Created with Microsoft Publisher 2016).*

2.1.1. The Transmission with the Support of the Standard IRS Model (IRS)

Discrete elements N exist in the standard IRS model (IRS), as shown in Figure 1, where $h_{sr} \in \mathbb{C}^N$ represents the source-to-IRS deterministic channel, and $[h_{sr}]n$ the nth element; $h_{rd} \in \mathbb{C}^N$. This specifies the channel that must be specified for the IRS to communicate with the destination.

$$\Theta = \alpha diag\left(e^{j\theta 1}, \ldots, e^{j\theta N}\right) \tag{3}$$

where $\alpha \in [0,1]$ is the reflection coefficient at the fixed amplitude; $\theta_1, \theta_2, \ldots, \theta_N$, these are the phase-shift parameters that may be enhanced with IRS. The final destination's received signal within the IRS was calculated using the system model obtained in [28], which was previously used in [27,29,30], as in (4).

$$y_{IRS} = (h_{sd} + h_{sr}^T \Theta h_{rd})\sqrt{ps} + n \tag{4}$$

where using the same definitions for p, s, and n as used in the SISO case. With IRS-supported transmissions, channel estimation is non-trivial since the destination has perfect knowledge of the channels, and the phase-shift parameters can be enhanced. However, [31] describes some contemporary techniques. Specifically, the IRS-supported network has a channel capacity as in (5).

$$R_{\mathrm{IRS}}(N) = \max_{\theta_1,\ldots,\theta_N} log_2\left(1 + \frac{p|h_{sd} + h_{sr}^T \Theta \boldsymbol{h}_{rd}|^2}{\sigma^2}\right) \tag{5}$$

$$R_{\mathrm{IRS}}(N) = log_2\left(1 + \frac{p(|h_{sd}| + \alpha \sum_{n=1}^{N} |[h_{sr}]_n [h_{rd}]_n|)^2}{\sigma^2}\right) \tag{6}$$

The rate expression in (5) will be obtained from the carrying capacity of a channel generating additive white Gaussian noise for any Θ. Take note that the essential factor is $h_{sr}^T \Theta h_{rd} = \alpha \sum_{n=1}^{N} e^{j\theta n} [h_{sr}]_n [h_{rd}]_n$. Following the same standard procedure as in [32,33], the maximum rate, which represents the capacity, is achieved whenever the phase shifts are chosen as $\theta_n = arg\ (h_{sd}) - arg\ ([\boldsymbol{h_{sr}}]_n [\boldsymbol{h_{rd}}]_n)$ to make each term in the sum have the same phase as h_{sd}.

2.1.2. The Transmission with the Support of the Optimized IRS Model (IRS^o)

In this paper, we present an improved version of the IRS model; it is the (IRS^o) model (shown in Figure 1) utilizing one of the available optimization algorithms to surpass the performance and capabilities of the IRS.

The enhanced, as in the (7) diagonal matrix, shows the properties of the IRS^o, just like in the IRS, except for the value of N.

$$\Theta^o = \alpha diag\left(e^{j\theta 1}, \dots, e^{j\theta N^o}\right) \tag{7}$$

where N^o, are the N enhanced, phase-shifting variables that can be represented by $\theta_1, \theta_2, \dots, \theta_{N^o}$, these optimize through IRS^o. Furthermore, the final destination received the enhanced signal within IRS^o, will be as in (8).

$$y_{IRS}^o = (h_{sd} + h_{sr}^T \Theta^o h_{rd})\sqrt{p^o}s^o + n^o \tag{8}$$

where p^o, is the enhanced transmit power, s^o, is the unit-power information's enhanced signal, and the enhanced receiver noise will be represented by $n^o \sim \mathcal{N}c(0, \sigma^2)$. To analyze how the optimized model for the IRS affects the enhanced channel capacity in a network, we will use the expressions (9) and (10).

$$R_{IRS^o}^o(N^o) = \max_{\theta_1,\dots,\theta_{N^o}} log_2\left(1 + \frac{p^o|h_{sd} + h_{sr}^T \Theta^o h_{rd}|^2}{\sigma^2}\right) \tag{9}$$

$$R_{IRS^o}^o(N^o) = log_2\left(1 + \frac{p^o\left(|h_{sd}| + \alpha\sum_{n^o=1}^{N^o}|[h_{sr}]_{n^o}[h_{rd}]_{n^o}|\right)^2}{\sigma^2}\right) \tag{10}$$

Although the analysis in this paper simplifies by assuming deterministic channels, extending it to fading channels with complete channel information is straightforward. We need only consider predictions of the rate equations in (6) and (10). In light of this, all the conclusions also hold in this case.

2.2. Performance of Analytics

Here, we analyze the three achievable rates discussed in the previous section. Uniquely, the phases of the channel elements ignore only the amplitudes used in the expressions. From now on, the notation $|h_{sd}| = \sqrt{\beta_{sd}}, |h_{sr}| = \sqrt{\beta_{sr}}, |h_{rd}| = \sqrt{\beta_{rd}}$, and $\frac{1}{N}\sum_{n=1}^{N}|[h_{sr}]_n[h_{rd}]_n| = \sqrt{\beta_{IRS}}$, will be introduced as a means of brevity within the IRS. However, the same notations will have different values with the IRS^o compared to the IRS, as follows $|h_{sd}^o| = \sqrt{\beta_{sd}^o}, |h_{sr}^o| = \sqrt{\beta_{sr}^o}, |h_{rd}^o| = \sqrt{\beta_{rd}^o}$, and $\frac{1}{N^o}\sum_{n^o=1}^{N^o}|[h_{sr}^o]_{n^o}[h_{rd}^o]_{n^o}| = \sqrt{\beta_{IRS^o}^o}$, where these notations are used to represent the IRS^o. The equations (2), (6), and (10) must be reformulated for more compact forms.

$$R_{SISO} = log_2\left(1 + \frac{p\beta_{sd}}{\sigma^2}\right) \tag{11}$$

$$R_{IRS}(N) = log_2\left(1 + \frac{p\left(\sqrt{\beta_{sd}} + N\alpha\sqrt{\beta_{IRS}}\right)^2}{\sigma^2}\right) \tag{12}$$

$$R_{IRS^o}^o(N^o) = log_2\left(1 + \frac{p^o\left(\sqrt{\beta_{sd}^o} + N^o\alpha\sqrt{\beta_{IRS}^o}\right)^2}{\sigma^2}\right) \tag{13}$$

Equality will be obtained for $N = 0$ with the IRS and for $N^o = 0$ with IRS^o, where $R_{IRS}(N)$ is an increasing function of N, while $R_{IRS^o}^o(N^o)$ is an increasing function of N^o. It is evident that $R_{IRS^o}^o(N^o) > R_{IRS}(N) \geq R_{SISO}$. As mentioned in [29] and elaborated on in [27,34], the rate increases as $\mathcal{O}(log_2(N^2))$ when N becomes large. For this reason, for values of N, the exponential growth rate presented in this paper is $\mathcal{O}\left(log_2\left(N^{o2}\right)\right)$. Consequently, it is not simple to evaluate the two cases of the IRS and the IRS^o.

The radio transmission will work enhanced within this paper's (IRS^o) model compared to the IRS described in the previous literature. The transmission supported by the (IRS^o) model has the highest rate for any $N > N^o \geq 1$ if $\beta_{sd} > \beta_{sd}^o > \beta_{sr}^o$; because the IRS-supported transmission provides the highest rate for $N \geq 1$ if $\beta_{sd} > \beta_{sr}$ compared

to transmissions supported with any additional communications equipment [27], in which the IRS^o model achieves the highest rate in the case of $\beta_{sd}^o \leq \beta_{sr}^o < \beta_{sd}$, while the IRS achieves the highest rate in the case of $\beta_{sd} \leq \beta_{sr}$.

$$N > \frac{\sqrt{\left(\sqrt{1+\frac{2p\beta_{rd}\beta_{sr}}{(\beta_{sr}+\beta_{rd}-\beta_{sd})\sigma^2}}-1\right)\frac{\sigma^2}{p}}-\sqrt{\beta_{sd}}}{\alpha\sqrt{\beta_{IRS}}} \tag{14}$$

$$N^o > \frac{\sqrt{\left(\sqrt{1+\frac{2p^o\beta_{rd}^o\beta_{sr}^o}{(\beta_{sr}^o+\beta_{rd}^o-\beta_{sd}^o)\sigma^2}}-1\right)\frac{\sigma^2}{p^o}}-\sqrt{\beta_{sd}^o}}{\alpha\sqrt{\beta_{IRS}^o}} \tag{15}$$

As for the distinction between the transmission supported by the (IRS^o) and IRS; the IRS supports the case that $R_{IRS}(N) > R_{SISO}$ for $N \geq 1$, yield the highest rate if $R_{\mathrm{IRS}}(N) > R_{ace}$; where any additional communications equipment will be represented by R_{ace}. Because the IRS supports multiple transmissions. $R_{SISO} > R_{ace}$ will cause this for $\beta_{sd} > \beta_{sr}$. As a consequence of this, the result will be $R_{IRS}(N) > R_{SISO} > R_{ace}$. But, this paper shows that, $R_{IRS^o}^o(N^o) > R_{SISO}$ for $N > N^o \geq 1$, in the case supported by the IRS^o, yields the highest rate if and only if $R_{IRS^o}^o(N^o) > R_{IRS}(N)$ achieves. Due to transmission supported by the IRS^o, $\beta_{\mathrm{sr}} > \beta_{sd}^o > \beta_{sr}^o$ always occurs when $R_{SISO} < R_{IRS}(N)$. Therefore, the result will be $(R_{IRS^o}^o(N^o) > R_{IRS}(N) > R_{SISO})$ in this case. It can reduce the inequality, $R_{IRS}(N) > R_{ace}$ by using (12), if the situation of $\beta_{sd} \leq \beta_{sr}$, with the IRS supporting the transmission. Furthermore, if the case of $\beta_{sd}^o \leq \beta_{sr}^o < \beta_{sd}$ transmission supported by the IRS^o, the inequality $R_{IRS^o}^o(N^o) > R_{IRS}(N)$ can be simplified by using (13).

A LOS between the IRS^o, and IRSs are required to interpret the results correctly IRS^o. Since any element in h_{sr} has the same magnitude as any element in h_{sr}, and any element in h_{rd} has the same magnitude as any element in (h_{rd}), it follows that the (IRS^o) elements all have the same magnitude as the essential IRS model elements. As a consequence of this, $\beta_{IRS} = \beta_{sr}\beta_{rd}$, and $\beta_{IRS}^o = \beta_{sr}^o\beta_{rd}^o$.

The higher rate of ($\beta_{sd} > \beta_{sr}$) is provided by transmissions supported by the standard model of the IRS, as in [27]. It is contrary to what is in this paper; the highest rate of $\beta_{sd} > \beta_{sr}$ is provided by transmissions supported by the optimized model of the IRS.

The difference between $R_{IRS}(N)$ and R_{SISO} is negligible for most actual values of N when the value is small for β_{rd}, since $\sqrt{\beta_{sd}} \gg N\alpha\sqrt{\beta_{IRS}} = N\alpha\sqrt{\beta_{sr}\beta_{rd}}$. However, the difference in this paper is between $R_{\mathrm{IRS}}(N)$, R_{SISO} and $R_{IRS^o}^o(N^o)$ is the smallest since $\sqrt{\beta_{sd}^o} \gg N^o\alpha\sqrt{\beta_{IRS}^o} = N^o\alpha\sqrt{\beta_{sr}^o\beta_{rd}^o}$ for most practical values of N^o while β_{rd}^o is the smallest number for the most practical values of $\beta_{rd}^o < \beta_{rd}$. It should be noted that in wireless communications, −50 dB is considered a "large" channel gain. In cases where $\beta_{sd} \leq \beta_{sr}$, an IRS can result in a noticeable performance improvement. Conversely, when $\beta_{sd}^o \leq \beta_{sr}^o < \beta_{sd}$, an ($IRS^o$) can offer a significantly better performance boost.

The coefficient α of the amplitude reflection, the channel gains β_{sd}, β_{sr}, and β_{rd}, and the transmit SNR p/σ^2 from the right-hand side of (14), where we recall that $\beta_{IRS} = \beta_{sr}\beta_{rd}$. It is noted of $p \to \infty$ (on the right) is essential $-\sqrt{\beta_{sd}}/\alpha\sqrt{\beta_{sr}\beta_{rd}}$ (on the left). However, the transmitted SNR p^o/σ^2, the coefficient α of amplitude reflection, and the enhanced channel gains $\beta_{sd}^o, \beta_{sr}^o$, and β_{rd}^o, determine the enhanced value on the right-hand side of (15), where we recall that $\beta_{IRS}^o = \beta_{sr}^o\beta_{rd}^o$. It noted $-\sqrt{\beta_{sd}^o}/\alpha\sqrt{\beta_{sr}^o\beta_{rd}^o}$ (on the right) gets close to $\beta_{IRS}^o = \beta_{sr}^o\beta_{rd}^o$ (on the left). It means that for each given, $p^o \to \infty$, the most significant rate at a high SNR (p/σ^2) is achieved by the transmission supported by the IRS for any N. Conversely, the inequality in (14) reduces to (16).

$$N > \frac{\sqrt{\frac{1}{(\beta_{sr}+\beta_{rd}-\beta_{sd})}}-\frac{\sqrt{\beta_{sd}}}{\sqrt{\beta_{sr}\beta_{rd}}}}{\alpha} \tag{16}$$

Also, for any (N^o), it stands to reason that the transmission with the (IRS^o) will transmit at the most significant rate when the SNR (p^o/σ^2), is high. Conversely, the inequality in (15) simplifies to (17).

$$N^o > \frac{\sqrt{\frac{1}{(\beta_{sr}^o+\beta_{rd}^o-\beta_{sd}^o)}}-\frac{\sqrt{\beta_{sd}^o}}{\sqrt{\beta_{sr}^o\beta_{rd}^o}}}{\alpha} \tag{17}$$

The numbers $p \to 0$ and $p^o \to 0$ have different values, given that $p \to 0$ achieved with $\beta_{sd} \leqslant \beta_{sr}$, while $p^o \to 0$ is achieved with ($\beta_{sd}^o \leqslant \beta_{sr}^o < \beta_{sd}$), it can result in huge numbers. As an illustration, if $\alpha = 1$, $\beta_{rd} = -60$ dB, $\beta_{sr} = -80$ dB, and $\beta_{sd} = -110\ dB$, the result is that (16) becomes $N > 963$.

Accordingly, the SNR and the number of elements determine whether a standard model for the IRS or an optimized model for the IRS is selected. It assumes throughout this study that both, β_{IRS} and $\beta_{IRS^o}^o$ are independent of N and N^o, respectively.

$$N^{opt(IRS)} = \sqrt[3]{\frac{(2^{R_d}-1)\sigma^2}{\alpha^2 \beta_{IRS} P_e}} - \frac{1}{\alpha}\sqrt{\frac{\beta_{sd}}{\beta_{IRS}}}. \tag{18}$$

$$N^{o\,opt(IRS^o)} = \sqrt[3]{\frac{(2^{R_d}-1)\sigma^2}{\alpha^2 \beta_{IRS^o}^o P_e}} - \frac{1}{\alpha}\sqrt{\frac{\beta_{sd}^o}{\beta_{IRS^o}^o}}. \tag{19}$$

In most cases, the ideal number of elements in Equations (18) and (19) is not a whole number. Hence, the closest integer, whether greater or smaller, can be used to approximate the true optimum. The SISO situation with N = 0 is the actual ideal value because the best value might potentially be damaging. So, $N^{opt(SISO)} = 0$.

Maximizing energy efficiency while adhering to data rate (R_d) limits may be accomplished with the assistance of the SISO, IRS, and IRS^o, as shown by the findings from [27], where EE of SISO (EE_{SISO}), EE of IRS (EE_{IRS}) and EE of IRS^o ($EE_{IRS^o}^o$) determined by Equations (20)–(22).

$$EE_{SISO} = R_d / P_{SISO}^{Total} \tag{20}$$

$$EE_{IRS} = R_d / P_{IRS}^{Total} \tag{21}$$

$$EE_{IRS^o}^o = R_d / P^{o\,Total}_{IRS^o} \tag{22}$$

where (P_{IRS}^{Total}), does the IRS use the total power in the system, and ($P^{o\,Total}_{IRS^o}$), does the IRS consume the total power in the system at the appropriate R_d. For example, P_{IRS}^{Total} consists of the combined hardware dissipation and transmit power. The conventional IIR model's calculations are given in (23) [27], whereas the optimized IIR model's calculations are given in (24).

$$P_{IRS}^{Total}(N) = \frac{p_{IRS}(N)}{\nu} + P_s + P_d + NP_e \tag{23}$$

$$P^{o\,Total}_{IRS^o}(N^o) = \frac{p^o{}_{IRS^o}(N^o)}{\nu} + P_s + P_d + N^o P_e \tag{24}$$

where $p_{IRS}(N)$ is the power required for transmission using the IRS as in (27), and $p^o{}_{IRS^o}(N^o)$ is the power required for transmission using the IRS^o model as in (28); furthermore, P_s and P_d indicate the hardware dissipated powers at the source and the destination, respectively. Power lost by the element as a result of the phase-shifting circuitry, denoted by P_e. $\nu \in [0,1]$ where the total power consumption of the SISO system (P_{SISO}^{Total}) determine as in (25), which determines the power amplifier's efficiency in the SISO situation.

$$P_{SISO}^{Total} = \frac{p_{SISO}}{\nu} + P_s + P_d \tag{25}$$

where the power necessary to provide a R_d, in the SISO case, the standard IRS model and (IRS^o) models are determined by (26), (27), and (28), respectively.

$$p_{SISO} = (2^{R_d} - 1)\frac{\sigma^2}{\beta_{sd}} \tag{26}$$

$$p_{IRS}(N) = (2^{R_d} - 1)\frac{\sigma^2}{\left(\sqrt{\beta_{sd}} + N\alpha\sqrt{\beta_{IRS}}\right)^2} \tag{27}$$

$$p^o{}_{IRS^o}(N^o) = (2^{R_d} - 1)\frac{\sigma^2}{\left(\sqrt{\beta_{sd}^o} + N^o\alpha\sqrt{\beta_{IRS^o}^o}\right)^2} \tag{28}$$

Suppose the destination demands a particular R_d. Then, suppose we use the formulas for the $R_d s$ in (11), (12), and (13). In that case, we can determine the transmission power requirements for each of the three possible communication setups.

Consequently, (22) is a non-convex optimization problem for the IRS. Since this optimization problem is non-convex, there is no conventional solution. Consequently, in this paper, we propose a novel artificial intelligence algorithm based on the DS-PSO technique, which will be discussed in the next section.

2.3. The Proposed AI Algorithm to Improve Performance

At (27), the IRS addresses the non-convex optimization problem via an AI algorithm based on the DS-PSO technique. It is a hybrid particle swarm optimization algorithm integrating both static and dynamic techniques. The traditional Particle Swarm Optimization (PSO) approach utilizes a search space to initiate the particle swarm. Each particle is assigned a swarm subset, neighborhood, velocity, and a random position to monitor the swarm's particles. In each iteration, every particle in the algorithm evaluates its present functional condition. Once the fitness of the current solution exceeds that of the particle's current personal best (Pos_{best}), the current position is deemed the new personal best (Pos_{best}). The particle's position and velocity are updated utilizing Equations (31) and (29) provided below. DS-PSO has a notable similarity to PSO algorithms since it amalgamates the topologies of both static and dynamic iterations of traditional PSO.

The distinguishing feature of DS-PSO is the implementation of two distinct topologies for particles: one for their dynamic neighborhood and another for their static neighborhood. Conversely, the additional dynamic designs prioritize exploration of the search space rather than early convergence. A completely random topology is generated concurrently with the execution of the operation. Conversely, alternative dynamic PSO algorithms lose the exploitative characteristics of traditional PSO while employing static topologies.

Swarm particles are modifying their velocities (V) and positions (Pos) in accordance with Equations (30) and (31), influenced by the neighborhood bests (N_{pbest}) across all topologies of the DS-PSO.

$$\begin{aligned} Vel_{par}(i) = C_c[Vel_{par}(i-1) \\ +C_1R_1\left(Pos_{par}(i-1) - X_{par}(i-1)\right) \\ + C_2R_2\left(Nei_{parbest}(i-1) - X_{par}(i-1)\right) \end{aligned} \tag{29}$$

$$\begin{aligned} V_{par}(i) = C_c[V_{par}(i-1) \\ +C_1R_1\left(Pos_{par}(i-1) - X_{par}(i-1)\right) \\ + C_2R_2\left(D_{parbest}(i-1) - X_{par}(i-1)\right) \\ + C_3R_3\left(S_{parbest}(i-1) - X_{par}(i-1)\right)] \end{aligned} \tag{30}$$

$$X_{par}(i) = X_{par}(i-1) + V_{par}(i) \tag{31}$$

The velocity is denoted as $V_{par}(i)$ in the preceding equations, whereas $X_{par}(i)$, signifies the particle's (par) position at the current iteration. The particle, individual, dynamic, and static enhanced solutions identified to date in iteration (i) are denoted by $Pos_{par}(i)$, $D_{parbest}(i)$ and $S_{parbest}(i)$.

The fundamental novelty of the DS-PSO algorithm, and its key difference from existing optimization approaches like standard PSO or Genetic Algorithms (GA), lies in its hybrid topology. Traditional PSO relies on a single social network (e.g., a global best), which often leads to premature convergence in complex, multi-modal problems like IRS phase-shift optimization. In contrast, DS-PSO simultaneously maintains two distinct social networks for each particle: a stable static topology ($S_{parbest}$) that preserves reliable social information and promotes consistent exploitation, and a randomly changing dynamic topology ($D_{parbest}$) that injects novelty into the search process, preventing stagnation in local optima. This hybrid strategy is specifically designed to achieve a superior balance between exploration (searching new areas of the solution space) and exploitation (refining known good solutions). While other algorithms force a choice between these two competing goals, DS-PSO adapts its search behavior organically; this makes it uniquely suited for the high-dimensional, non-convex optimization problem posed by IRS, where finding the global optimum phase-shift configuration is paramount for maximizing energy efficiency.

The hybrid nature of DS-PSO, combining both static $S_{parbest}(i)$ and dynamic $D_{parbest}(i)$ Social topologies are its key adaptive strength. This design directly addresses a core challenge in metaheuristics: the trade-off between exploration (searching new areas) and exploitation (refining known good areas). A purely static topology (e.g., a ring structure) excels at exploitation, promoting stable convergence but potentially causing premature convergence to a local optimum in complex, multi-modal problems like IRS phase-shift optimization. Conversely, a purely dynamic topology (e.g., randomly changing neighbors each iteration) is highly explorative but can lack direction, leading to slow and unstable convergence.

DS-PSO adapts by not forcing a choice between these two strategies. The static topology provides a foundation of reliable, long-range social information, ensuring consistent guidance and preventing chaotic behavior. Simultaneously, the dynamic topology injects randomness and novelty into the search process, allowing particles to escape local optima by receiving guidance from different, randomly assigned neighbors. The acceleration coefficients intrinsically govern the algorithm's behavior (C_1, C_2 and C_3). In scenarios where the fitness landscape is simpler and convex, the consistent guidance from the static component (C_3) will dominate, leading to fast and stable convergence. In highly complex, non-convex scenarios like our IRS optimization problem, the explorative force of the dynamic component (C_2) becomes more critical, enabling the swarm to discover superior phase-shift configurations that a purely static approach might miss.

The constriction coefficient, C_c, is typically set at roughly 0.7298438 to mitigate explosive velocities. The acceleration coefficients C_1 and C_2, utilized in Equation (29), augment the attraction of particles to Pos_{par} and $N_{parbest}$, respectively. The total acceleration coefficient for standard PSO is 4.1, with individual coefficients, C_1 and C_2 being equal to 2.05. Additionally, the acceleration coefficients C_1, C_2 and C_3 are employed in Equation (30) to augment the attraction of particles to $Pos_{par}(i)$, $D_{parbest}(i)$ and $S_{parbest}(i)$, respectively. Every particle will achieve optimal static, dynamic, and individual performance. As a result, DS-PSO identifies three acceleration coefficients, in contrast to the two identified by the traditional PSO algorithm. Alongside being established at 4.1/3, the acceleration coefficients, (C_1, C_2 and C_3), each produces a value of 1.366666667.

The components of the velocity equation are multiplied by a vector of randomly generated values, R_1, R_2, and R_3, which are constrained within the interval [0,1] to facilitate research. Particles must be confined within the search space, delineated by the interval [V_{min}; V_{max}], where [V_{min}; V_{max}] represents the minimum and maximum values of the search space, and each element of V_{par} must reside within this range. The particle exhibits a preference for $D_{parbest}$ and $S_{parbest}$, over $N_{parbest}$, the optimal neighbors. Therefore, while evaluating the static and dynamic topologies of particles, this is the ideal solution [35–37].

The pseudocode flow of the sequence of operations of the DS-PSO algorithm is shown in [37] as a reference for implementation details.

Below is a pseudocode that visually represents the dual influence of static and dynamic topologies in DS-PSO. This format is designed to provide a step-by-step guide to the DS-PSO algorithm's operation. The pseudocode has been streamlined to focus on explaining the intuition behind the hybrid topology and the key equations for IRS Phase-Shift Optimization, where it illustrates the process flow.

DS-PSO Algorithm: Structured Pseudocode

Algorithm: DS-PSO for IRS Phase-Shift Optimization

Inputs:

- *par*: **Number of particles in the swarm**
- ***f*: Objective function (e.g., to maximize Energy Efficiency, EE)**
- $\boldsymbol{max_{Iter}}$**: Maximum number of iterations**
- $\boldsymbol{P_{restructure}}$**: Probability of restructuring dynamic neighborhoods**
- $\boldsymbol{V_{min}}$**;** $\boldsymbol{V_{max}}$**: Minimum and maximum velocity in the search space**

Outputs:

- $\boldsymbol{S_{parbest}}$**: Global best position found (optimal phase-shift configuration)**
- $\boldsymbol{f(S_{parbest})}$**: Best objective function value (maximized EE)**

Initialization:

1. **For each particle** $\boldsymbol{i}$ **= 1 to** ***par*:**

- **Initialize position** $\boldsymbol{X_{par}(i)}$ **randomly within the search space [**$\boldsymbol{V_{min}}$**;** $\boldsymbol{V_{max}}$**].**
- **Initialize velocity** $\boldsymbol{V_{par}(i)}$**= 0.**

- **Initialize personal best position;**

$$\boldsymbol{Pos_{par}(i) = X_{par}(i).}$$

- **Evaluate personal best fitness f($\boldsymbol{Pos_{par}(i)}$).**

2. **Initialize static topology (e.g., Ring) for all particles to define $\boldsymbol{S_{parbest}(i)}$.**
3. **Initialize the dynamic topology by randomly assigning $\boldsymbol{D_{parbest}(i)}$, for each particle.**
4. **Initialize global best $\boldsymbol{S_{parbest}}$.**

Main Loop:

1. **for iteration = 1 to $\boldsymbol{max_{Iter}}$ do**
2. **for each particle $\boldsymbol{i}$ do**
3. **Evaluate the fitness f($\boldsymbol{X_{par}(i)}$)**
4. **if f($\boldsymbol{X_{par}(i)}$) is better than f($\boldsymbol{Pos_{par}(i)}$) then**
5. **Update personal best: $\boldsymbol{Pos_{par}(i) = X_{par}(i)}$**
6. **end if**
7. **Identify the static neighborhood best $\boldsymbol{S_{parbest}(i)}$, from the static topology.**
8. **Identify the dynamic neighborhood best $\boldsymbol{D_{parbest}(i)}$, from the dynamic topology.**
9. **Update Velocity using Equation (30):**
10. **Bound $\boldsymbol{V_{par}(i)}$ within $\boldsymbol{[V_{min}; V_{max}]}$.**
11. **Update Position using Equation (31):**
12. **Bound $\boldsymbol{X_{par}(i)}$, within the search space.**
13. **end for (particle loop)**
14. **if $\boldsymbol{rand() < P_{restructure}}$ then**
15. **Restructure all dynamic topologies (randomly reassign $\boldsymbol{D_{parbest}}$ for each particle.)**
16. **end if**
17. **Update the global best solution $\boldsymbol{S_{parbest}}$.**
18. **end for (iteration loop)**

Return $S_{parbest}, f(S_{parbest})$

Table 1. The main parameters used in the DS-PSO algorithm.

Parameter	Value
Iteration (i)	1000
Particles (par)	10
coefficients of acceleration ($C_1 = C_2 = C_3$)	4.1/3
The minimum probability of restructuring neighborhoods	0.1
The maximum probability of restructuring neighborhoods	0.2
Intervals for the probability of restructuring neighborhoods	0.5
Intertie coefficient (spaced frequency points)	1
The search space's minimum values (V_{min})	1
Maximum values in the search space (V_{max})	70

Traditional PSO uses a single social topology (e.g., a global best) to guide the swarm; this can lead to premature convergence in complex problems like IRS phase-shift optimization, where the search space is highly multi-modal. The DS-PSO algorithm hybridizes this approach by maintaining two distinct social networks for each particle: a *static* topology (e.g., a ring or star structure) that preserves stable, long-range social information and promotes exploration, and a *dynamic* topology that randomly changes neighbors over iterations, preventing premature stagnation.

In the context of optimizing an IRS with N elements, each particle's position represents a candidate set of phase shifts ($\theta_1, \theta_2, ..., \theta_N$). A traditional PSO might get trapped in a local optimum, failing to find the best possible phase configuration to maximize the SNR at the destination. In contrast, the dynamic component of DS-PSO allows a particle

to occasionally receive guidance from a random, different part of the swarm, effectively 'jumping' out of a local valley. The static component ensures it still follows a consistent, proven path from its stable neighbors. This hybrid strategy is particularly effective for IRS optimization, as it balances the need for a thorough search of the vast phase-shift space (exploration) with the need to refine and converge on the best-found solution (exploitation).

3. Results

This section presents the simulation results and comparative performance analysis of the proposed AI-optimized IRS model against benchmark systems, evaluating key metrics such as energy efficiency and data rate across various operational regimes.

This section assesses the appropriateness of approximate outcomes to determine the selection between a standard IRS model and an (IRS^o) model. It determines whether the experimental setups employed in Section 2 function in the high or low SNR regime. A numerical analysis of the systems will be conducted. Subsequently, the EE of the transmission aided by the model of (IRS^o) is computed using the mathematical equations mentioned in Section 2 of this paper. A comparative analysis is then conducted with the findings of previous research studies.

3.1. Transmit Destination

The 3GPP Urban Micro (UMi) model, as described in reference [38], is employed with the carrier frequency set at 3 GHz to depict the channel gains accurately. The line-of-sight (LOS) and non-line-of-sight (NLOS) versions of UMi, specified for distance $\geq$ 10 m, are used. Let us say that the antenna gains for the transmitter and receiver, measured in dBi, are G_t and G_r, respectively. It is possible to use UMi at both LOS and NLOS distances.

For the simulations in this study, we assume that the transmitter and receiver antennas (G_t and G_r) located between the source and the IRS have equal gains of 5 decibels of isotropic radiated power (dBi) within a distance of 100 m while disregarding shadow fading. Upon reaching the desired destination, the individual possesses a telephone with an omnidirectional antenna with a gain of 0 dBi.

The transmission in wireless communication networks is influenced by channel gain and distance factors. A detailed channel gain and distance diagram was designed to investigate and simulate a wireless communication system with an IRS. This diagram can be seen in Figure 2 for the wireless communication system supported by the IRS. The proposed communication system model, designed in this paper, is similar to the model presented in Figure 2. However, it utilizes the improved IRS model instead of the standard IRS model and adopts the improved LOS. Figure 2 depicts the stationary positions of both the source and the IRS or (IRS^o) proposed in this study. The simulations for this study assume the distances between the source and the standard IRS or IRS^o, as depicted in Figure 2, respectively. The proposed distance between the source and the IRS d_1 is 70 m. The user/destination can be located within the range of the source as long as the distance between them (d_2) is greater than or equal to 10.

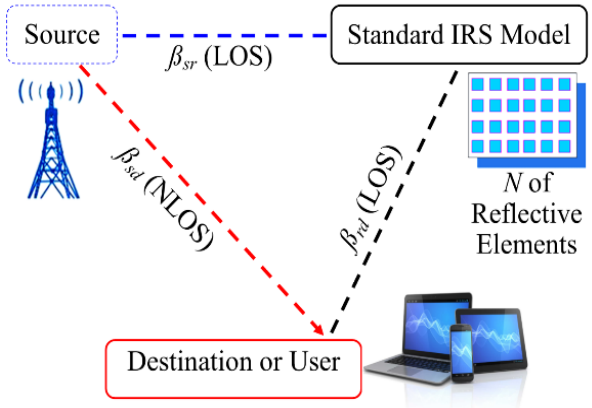

Figure 2. destination variables (d_1) and (d_2) for the simulation setup of the standard IRS model. *(Created with Microsoft Publisher 2016).*

Figure 2 shows the support of the IRS in facilitating transmission within the wireless communication system through the generation of line-of-sight (LOS) channels. A standard LOS version generates two distinct line-of-sight (LOS)

channels. The LOS between the source and the IRS is denoted as β_{sd}, while the LOS between the IRS and the user or destination is denoted as β_{rd}. Conversely, the NLOS version between the source and the user or destination generates a channel denoted as β_{sd}. The Equation $\beta_{IRS} = \beta_{sr}\beta_{rd}$ is used to represent the relationship between β_{IRS}, β_{sd}, and β_{rd}.

The presence of a weak channel gain between the source and the user or destination in the NLOS version necessitates the implementation of IRS for facilitating the transmission within next-generation wireless communication networks. The IRS produces LOS channels that offer superior performance compared to NLOS channels. Furthermore, as the distances increase, the channel gain values with LOS decrease, although they remain superior to those with NLOS; this resulted in the utilization of LOS properties in the design of a wireless communication system facilitated by implementing an IRS, resulting in significant advantages.

Consequently, the utilization of IRS in wireless communication networks has resulted in the generation of two LOS channels. One channel exists between the source and the IRS. In contrast, the other channel exists between the IRS and the user or destination, leading to enhanced transmission performance in these networks.

The LOS channels within the model of (IRS^o) will consist of two channels. The initial channel connecting the source and the model of IRS^o is denoted as β_{sr}. This channel's channel is optimized by maximizing the LOS between the source and the (IRS^o), denoted as β_{sr}. The second channel between the (IRS^o) and the user or destination is created by optimizing the LOS channel between the (IRS^o) and the user or destination, denoted as β_{rd}. The Equation can be simplified as $\beta^o_{IRS^o} = \beta^o_{sr}$ and β^o_{rd}.

The initial step in the simulation involves calculating the channel gain value (β_{sd}) for the SISO case in the communication system depicted in Figure 2. This calculation uses Equation (32) due to its NLOS nature. The channel gains values (β_{rd} and β_{sr}) with the standard IRS of the communication system in Figure 2 can be calculated using Equation (32). These values are determined based on the distance d1 and the antenna gains (G_t, and G_r), between the source and the IRS; this is to determine the values of β_{sd} and β_{sr}. Furthermore, the channel gain values (β^o_{sr} and β^o_{rd}) are calculated using Equation (33) for the proposed (IRS^o) model for the communication system. The channel gain using the improved IRS is the improved LOS version.

$$\beta(d)[dB] = G_t + G_r + \begin{cases} -37.5 - 22\,log_{10}\left(\frac{d}{1\ m}\right) & if\ LOS \\ -35.1 - 36.7\,log_{10}\left(\frac{d}{1\ m}\right) & if\ NLOS \end{cases} \tag{32}$$

$$\beta^o(d)[dB] = Optimized\ [G_t + G_r + \{-37.5 - 22\,log_{10}\left(\frac{d}{1\ \mathrm{m}}\right)\}] \quad if\ Optimized\ LOS \tag{33}$$

Given the superior performance of the optimized LOS version compared to the standard LOS version, it is plausible to anticipate that the proposed design of the IRS model in this research paper may yield improved performance compared to the standard IRS model. Thus, this study's proposed (IRS^o) can enhance the performance of 6G communication systems. This claim can be supported in this paper by using an IRS system performance evaluation measure. Therefore, this paper suggests implementing (energy efficiency compared to data rate) evaluation measures for IRS systems, specifically focusing on the standard IRS model and the proposed (IRS^o) model that is optimized in this paper. A comparative analysis is then performed to compare the findings of this research with previous studies on (energy efficiency compared to data rate) in alternative IRS models.

3.2. Energy Efficiency Compared to Data Rate

The simulation involves evaluating the performance of the SISO case, the standard IRS model, and the proposed (IRS^o) model based on their energy efficiency. In this paper, we determined the parameters associated with energy efficiency, including the quantity of the data rate, which is attributed to the significance of these parameters in enhancing the performance of the IRS. In this section, we aim to calculate energy efficiency values using the parameters from Table 2.

Table 2. The parameters for simulation in this paper.

Parameter	Value
Bandwidth (B)	10 MHz
Carrier frequency (FC)	3 GHz

Noise figure	10 dB
Noise power	-94 dBm
Power spectral density of noise	-174 dBm/Hz
α	1
Range of data rate (R_d)	[0 10]
The source's transceiver hardware power dissipation (P_s)	100 mW
Dissipation of power in the destination's transceiver hardware (P_d)	100 mW
The dissipation of power per IRS element (mw) (P_e)	5 mW
Power amplifier efficiency at the source (v)	0.5
Range of distance (d)	70 m
Distance (d_1) between the source and IRS/IRS^o	70 m
The minimum distance (d_2), between the source and destination	10 m

In the simulations in this paper, we will use the proposed algorithm, in addition to using the LOS version mentioned in Section 5.1, which was improved.

Simulations were performed for the SISO case, the standard IRS model, and the proposed IRS model that is optimized in this study. The simulations compared energy efficiency in terms of data rate. Next, the findings of this study will be compared to previous research on energy efficiency concerning data.

Calculating energy efficiency requires determining the total transmission power, which in turn requires calculating the required transmission capacity and the number of elements within the IRS. Calculating the number of elements required within the IRS involves determining the channel gain values of the IRS, which serves as evidence of the channel gain value. (β_{rd} and β_{sr}) related to the IRS are essential in determining the number of reflective elements within the IRS. Therefore, we sought to use improved channel gain values. The proposed algorithm relates (β_{sr}^{o} and β_{rd}^{o}) to the (IRS^{o}) proposed in this paper.

To obtain the results of this study, the energy efficiency values for the SISO case, the standard IRS, and the (IRS^{o}) proposed in this paper are calculated using Equations (20)–(22), respectively. To determine the total transmission power values for the SISO cases, the standard IRS, and the (IRS^{o}) proposed in this paper, Equations (23)–(25) are utilized, respectively. The power requirements for each SISO case are calculated, including the standard IRS and the (IRS^{o}) proposed in this paper, using Equations (26)–(28), respectively. The number of reflective elements in both the standard IRS and the (IRS^{o}) proposed in this study can be determined using Equations (18) and (19). It is worth mentioning that the number of reflective elements in the SISO case is zero. The channel gains (β_{rd} and β_{sr}) with the standard IRS of the communication system depicted in Figure 2 was determined using Equation (32). The channel gains values (β_{sr}^{o} and β_{rd}^{o}) with the (IRS^{o}). The performance of the communication system was determined using Equation (33). The channel gain values obtained from Equations (32) and (33) are included in Equations (18) and (19), respectively.

This study conducted simulations to evaluate the energy efficiency values for three cases: SISO, IRS standards, and (IRS^{o}) proposed in this paper. As such, the simulations in Section 5.2 of this study formulated the energy efficiency values concerning data rate.

This study conducts a comparative analysis of energy efficiency values concerning data rates. Based on the simulations conducted in this study, the energy efficiency values concerning data rates for the SISO case, standard IRS, and (IRS^{o}) proposed in this paper are shown in Table 3 and Figures 3 and 4.

Table 3 and Figure 4 reveal that the proposed (IRS^{o}) model underperforms the SISO and standard IRS models at very low data rates (e.g., R_d = 0.01 and 2 bit/s/Hz); this is not an artifact of the optimization algorithm but a fundamental system trade-off. At minimal data rates, the required transmit power is very low. The static hardware power dominates the total power consumption in an IRS-assisted system (P_s, P_d) and the power dissipated by the IRS elements (NP_e), as defined in Equations (23) and (24). The energy efficiency (EE) metric, defined as bits transmitted per Joule, is thus low because the denominator (total power) is significant even though the numerator (data rate) is small. A SISO system, with zero IRS elements (N = 0), has a lower total power overhead at these low rates and thus achieves a comparable or slightly higher EE. The DS-PSO algorithm correctly optimizes for this regime by effectively 'turning off' the IRS benefit when it is not needed. The superior performance of models like PSO-IRS and GA-IRS [32] at R_d = 0.01 is likely due to a different system model or cost function that does not penalize the IRS's hardware power consumption as heavily.

The model of (IRS^{o}) achieves increasing EE with data rate, while SISO and standard IRS models degrade after a peak, as shown in Figure 3.

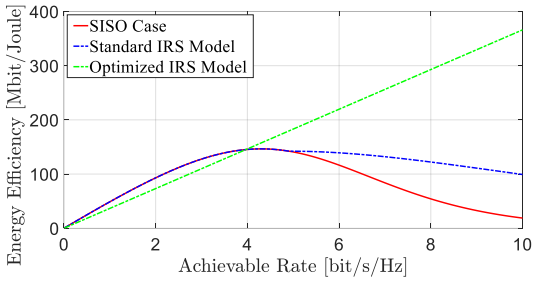

Figure 3. Energy efficiency compared to the data rate (R_d) function. *(Created with MATLAB R2023a).*

Figure 3 shows the energy efficiency values ranging from 0 to 400 Mbit/Joule and the data rate values ranging from 0 to 10 bit/s/Hz. These values were observed for the SISO case and the standard and (IRS^o) models proposed in this study. The energy efficiency index of the proposed (IRS^o) consistently increased as the data ratio increased. In contrast, the indicators for the standard IRS model and the SISO status decreased as the data ratio increased. Figure 4 was created to analyze the data in Figure 3 based on three cases: the SISO case, the standard IRS model, and the proposed (IRS^o) model.

There are sampled data points from Figure 3, highlighting the IRS^o's superior performance at data rates > 4 bit/s/Hz and its lower performance at very low rates due to hardware power overhead, as shown in Figure 4.

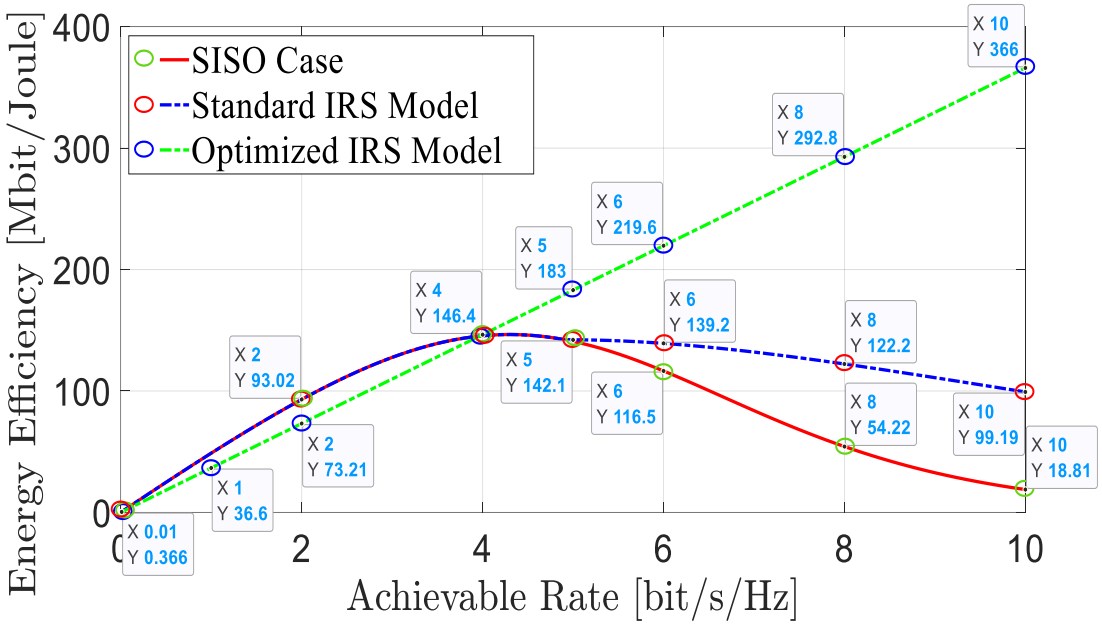

Figure 4. Energy efficiency values compared to data rate values. *(Created with MATLAB R2023a).*

Figure 4 shows the sampling of energy efficiency indicators in three cases: the SISO case, the standard IRS model, and the proposed (IRS^o) model. The purpose is to determine the energy efficiency values and data rate accurately. Seven samples were collected at (0.1, 2, 4, 5, 6, 8, and 10) bit/s/Hz of data rate.

The performance trade-off and the superior high-rate performance of the (IRS^o) model, as demonstrated in Table 3.

Table 3. The comparison between energy efficiency values concerning data rate values.

Range No. of R_d	**Range 1**	**Range 2**	**Range 3**	**Range 4**			
Sample No. of R_d	Sample 1	Sample 2	Sample 3	Sample 4	Sample 5	Sample 6	Sample 7
Data rate R_d	0.01	2	4	5	6	8	10

EE with SISO	0.366	93.02	146.4	142.1	116.5	54.22	18.81
EE with IRS	0.366	93.02	146.4	142.1	139.2	122.2	99.19
EE with Optimized IRS (IRS^o)	0.366	73.21	146.4	183	219.6	292.8	366

Table 3 was created based on the energy efficiency values and the proportion of data obtained from the energy efficiency indicators in Figure 4. Table 3 compares energy efficiency values for three cases: the SISO case, the standard IRS model, and the proposed (IRS^o) model. The comparison is conducted on specific data with energy efficiency measured in Mbit/Joule and data rate measured in bit/s/Hz.

It was essential to divide the data into five distinct ranges proportionately to analyze the data in Figure 4 and Table 3. The data rate can be categorized into five ranges: the first range corresponds to a data rate of 0.0; the second range encompasses data rates greater than 0.01 bit/s/Hz but less than 4 bit/s/Hz; the third range corresponds to a data rate of 4 bit/s/Hz; the fourth range includes data rates greater than 4 bit/s/Hz, and the fifth range encompasses data rates greater than 4 bit/s/Hz but less than or equal to 5 bit/s/Hz. Two ranges with equal energy efficiency values are observed in all three cases: the SISO case, the standard IRS model, and the proposed (IRS^o) model. These ranges, namely the first and third ranges, have distinct energy efficiency values from each other. The energy efficiency value is 0.366 Mbit/Joule with a data rate of 0.01 bit/s/Hz and increases to 146.4 Mbit/Joule with a data rate of 4 bit/s/Hz.

In the second range, when the data rate is between 0.01 bit/s/Hz and 4 bit/s/Hz, the energy efficiency values are the same for both the SISO case and the standard IRS model without the proposed (IRS^o) model. The energy efficiency values fall within the range of 0.366 Mbit/Joule to 146.4 Mbit/Joule, depending on the data rate values. In the scenario where a sample is taken from the second range at a data rate of 2 bit/s/Hz, it was observed that the energy efficiency of the proposed (IRS^o) model is lower compared to the energy efficiency of both the SISO case and the standard IRS model. Therefore, the findings of this study suggest that the proposed (IRS^o) exhibits low energy efficiency with low data rates.

In contrast, in the fifth range (data rate > 4 bit/s/Hz and ≤ 5 bit/s/Hz), the energy efficiency values are the same for both the SISO case and the standard IRS model without the proposed (IRS^o) model. Therefore, the energy efficiency value falls between 142.1 Mbit/Joule and 146.4 Mbit/Joule, depending on the specific data rate values. In the scenario where a sample is taken from the fifth range with a data rate of 5 bit/s/Hz, it was observed that the energy efficiency of the proposed (IRS^o) model is 183 Mbit/Joule. This value surpasses the energy efficiency observed in the SISO case and the standard IRS model. The results suggest that this study's proposed (IRS^o) model achieves high energy efficiency with a high data rate.

In the fourth range, where the data rate exceeds four bit/s/Hz, it is observed that the energy efficiency values differ among the three cases: the SISO case, the standard IRS model, and the proposed IRS model that is optimized in this study. When four samples are taken from the fourth range of the data rate (5, 6, 8, and 10) bit/s/Hz, it is observed that the energy efficiency decreases for both the SISO case and standard IRS models as the data rate increases. In contrast, it is observed that the energy efficiency of the proposed (IRS^o) in this study exhibits an upward trend as the data rate increases. Accordingly, the energy efficiency limit was highest among the SISO case, the standard IRS model, and the proposed (IRS^o) model, based on the samples in the fourth range, at a data rate of 10 bit/s/Hz. The energy efficiency results for different cases at a data rate of 10 bit/s/Hz were as follows: 18.81 Mbit/Joule for SISO, 99.19 Mbit/Joule for the standard IRS model, and 366 Mbit/Joule for the proposed (IRS^o) model.

If the data rate exceeds 4 bit/s/Hz, the energy efficiency of this study's proposed (IRS^o) is higher than the energy efficiency of the SISO case and the standard IRS model. The findings of this study suggest that the proposed (IRS^o) has superior energy efficiency at higher data rates.

To analyze the data in Table 4, we designed Figure 5, aiming to enhance data analysis. Table 4 shows an analytical comparison of energy efficiency versus data rate for the SISO systems and different IRS models, which are the standard model, the improved model in this study, models improved by the PSO algorithm, and the Genetic algorithm (GA) in [40], and single, dual, and triple IRS models in [39]. This analysis evaluates the performance of SISO, standard IRS, and IRS^o models in comparison to previous studies, focusing on the tradeoff between data rate (R_d) and energy efficiency. The results from Table 4 highlight the impact of IRS optimization techniques and provide insights into the scalability of multi-IRS configurations.

Table 4. Energy Efficiency (EE) vs. Data Rate (R_d) for SISO, Standard IRS, Optimized IRS (IRS^o) Model in this study, and IRS Models in Previous Studies.

Data Rate (R_d) [bit/s/Hz]	EE with SISO [Mbit/Joule] [in This Study]	EE with Standard IRS [Mbit/Joule] [in This Study]	EE with Single-IRS [Mbit/Joule] [39]	EE with Double-IRS [Mbit/Joule] [39]	EE with Triple-IRS [Mbit/Joule] [39]	EE with PSO-IRS [Mbit/Joule] [40]	EE with GA-IRS [Mbit/Joule] [40]	EE with Optimized IRS [Mbit/Joule] [in This Study]
0.01	0.366	0.366	0.366	0.366	0.366	44	44	0.366
2	93.02	93.02	20	34	50	42	42	73.21
4	146.4	146.4	40	68	100	EE < 25	EE < 25	146.4
5	142.1	142.1	50	85	125	EE < 15	EE < 15	183
6	116.5	139.2	60	102	150	EE < 10	EE < 10	219.6
8	54.22	122.2	80	136	200	EE < 5	EE < 5	292.8
10	18.81	99.19	100	170	250	0.5	0.5	366

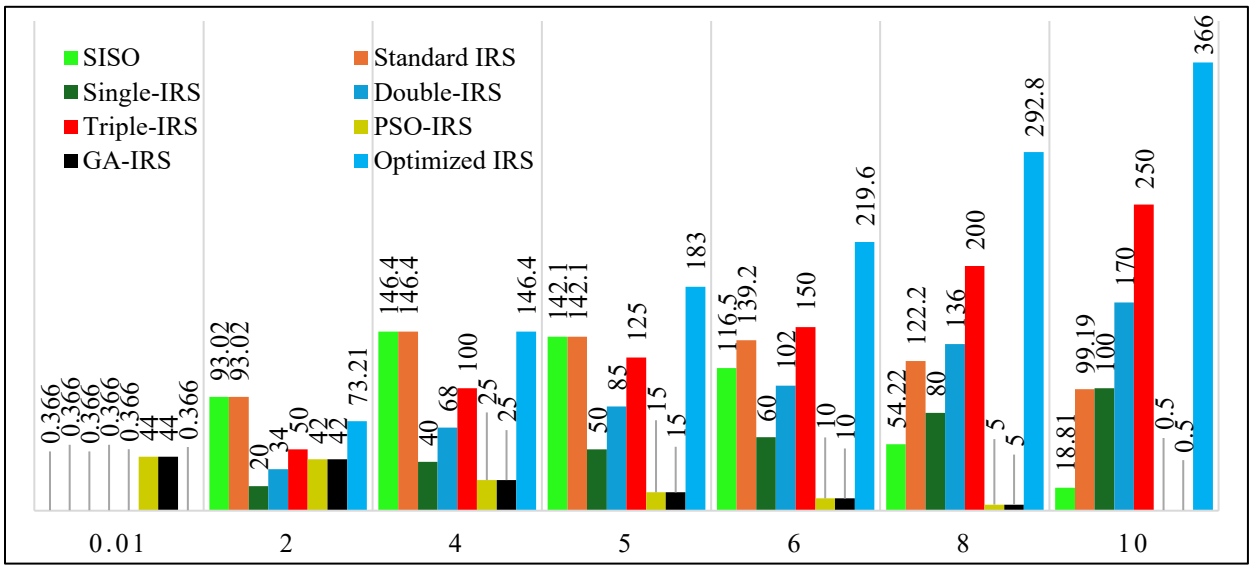

Figure 5. Energy efficiency compared to the data rate for (SISO, Standard IRS, Optimized IRS (IRS^o) Model in this study and IRS Models in Previous Studies. *(Created with Microsoft Excel 2016).*

Low Data Rate Regime ($R_d \leq 0.01$ bit/s/Hz): At extremely low data rates, all models (SISO, standard IRS, proposed IRS^o, IRS models improved by the PSO algorithm and the GA algorithm in [40], and single, dual, and triple IRS models in [39].) exhibit identical EE (~0.366 Mbit/Joule); this suggests that IRS deployment does not provide significant gains when the system operates at minimal throughput, likely due to negligible beamforming benefits at such low rates.

Moderate Data Rate ($2 \leq R_d \leq 6$ bit/s/Hz): The standard IRS matches SISO performance up to $R_d = 4$ bit/s/Hz, indicating no substantial improvement without optimization. The proposed IRS^o begins outperforming both SISO and standard IRS at $R_d = 5$ bit/s/Hz, achieving 183 Mbit/Joule compared to 142.1 Mbit/Joule for SISO. (Single/Double/Triple-IRS [39]) shows a linear increase in EE with R_d, but even the Triple-IRS (150 Mbit/Joule at $R_d = 6$) underperforms compared to the proposed IRS^o (219.6 Mbit/Joule). (IRS with PSO/GA, or PSO-IRS and GA-IRS [40]) shows high EE at very low R_d (44 Mbit/Joule at $R_d = 0.01$) but quickly degrades beyond $R_d = 2$, suggesting inefficiency in handling higher data rates.

High Data Rate ($R_d \geq 8$ bit/s/Hz): The proposed IRS^o demonstrates superior scalability, reaching 292.8 Mbit/Joule at $R_d = 8$ and 366 Mbit/Joule at $R_d = 10$, far exceeding all other models. Standard IRS shows moderate improvements over SISO, but remains significantly below the proposed (IRS^o). [39]'s Triple-IRS peaks at 250

Mbit/Joule at R_d = 10, still 32% lower than the IRS^o. [40]'s PSO-IRS and GA-IRS models fail to maintain competitive EE beyond R_d = 4, indicating limitations in high-throughput scenarios.

To quantify the superiority of the (IRS^o) model over other approaches, we calculate the percentage improvement in Energy Efficiency (EE) at different data rates based on Table 4. The results are summarized below:

IRS^o vs. SISO: The (IRS^o) underperforms SISO at R_d = 2 but dramatically improves at higher data rates (up to 1846% at R_d = 10); this suggests that IRS optimization is most effective in high-throughput scenarios.

IRS^o vs. Standard IRS: The IRS^o matches the standard IRS at low R_d. Nevertheless, provides significant gains (up to 269%) at higher rates; this confirms that optimization algorithms enhance IRS efficiency when data demand increases.

IRS^o vs. (Single/Double/Triple-IRS [39]): The IRS^o consistently outperforms [39]'s models by 46.4–266%. Notably, a single IRS^o surpasses even a Triple-IRS by 46.4%, proving that optimization is more impactful than adding more IRS layers.

IRS^o vs. (PSO-IRS and GA-IRS [40]): PSO-IRS and GA-IRS models perform exceptionally well at extremely low R_d (0.01) but collapse at higher data rates. The IRS^o dominates beyond R_d = 2, with >485% improvement at R_d = 4.

This analysis and comparison in Table 5 provides a clear understanding of the advancements made by the proposed (IRS^o) model in comparison to previous studies, highlighting its potential for future 6G communication systems.

Table 5. Overall superiority summary percentage improvement of optimized IRS (IRS^o) in this study over other models.

Comparison	Best Improvement (%)	Worst Case (%)
Optimized IRS (IRS^o) in this study vs. SISO in this study	+1846% (R_d = 10)	−21.3% (R_d = 2)
Optimized IRS (IRS^o) in this study vs. Standard IRS in this study	+269% (R_d = 10)	−21.3% (R_d = 2)
Optimized IRS (IRS^o) in this study vs. (Single-IRS [39])	+266% (all $R_d \geq 2$)	–
Optimized IRS (IRS^o) in this study vs. (Triple-IRS [39])	+46.4% (all $R_d \geq 2$)	–
Optimized IRS (IRS^o) in this study vs. (PSO-IRS and GA-IRS [40])	>+485% (R_d = 4)	−99.2% (R_d = 0.01)

Comparing the proposed (IRS^o) model in this paper, with competing models from previous studies regarding energy efficiency and data rate, indicates that the (IRS^o) model outperforms the competing models, and this model maintains high energy efficiency in the wireless communication system's transmission and receiving operations, even at high data rates. Also, it is the most effective model for enhancing transmission performance in sixth-generation communication networks. However, it can achieve a high data transmission rate of at least 10 Mbps while maintaining a high energy efficiency of at least 366 Mbit/Joule. Hence, we recommend applying the proposed method and (IRS^o) model in this study to enhance transmission performance in 6G networks with the aid of the IRS.

The simulation results presented in this study are based on the 3GPP Urban Micro (UMi) channel model, which provides a standardized and theoretically robust foundation for comparative analysis. However, it is important to acknowledge that this model, while useful, incorporates simplifications and may not fully capture the intricacies of real-world radio propagation environments, such as specific spatial correlations, intense scattering, or dynamic interference patterns. Therefore, to further strengthen the practical relevance of our findings, future work must prioritize validation in more complex and realistic scenarios.

4. Discussion

This section discusses the practical implementation challenges and limitations of the proposed AI-optimized IRS model, including channel estimation, hardware imperfections, and scalability, contextualizing the simulation results within real-world 6G deployment scenarios.

4.1. Channel Model Assumptions and Dynamic Environments

Our analysis utilizes deterministic flat-fading channels to derive closed-form expressions for data rate and energy efficiency, a common approach in foundational IRS literature [19,21] for tractability. We recognize that real-world environments are characterized by time-varying fading, shadowing, and blockages. The performance of an IRS is

contingent on accurate Channel State Information (CSI), and acquiring this in rapidly changing scenarios with mobile users is a significant challenge. The passive nature of IRS elements, which cannot transmit or receive pilot signals, further complicates channel estimation [16,23]. Future work must integrate robust channel estimation techniques and stochastic channel models (e.g., Rayleigh or Rician fading) to evaluate the resilience of our DS-PSO algorithm under uncertainty. The algorithm's dynamic topology component, designed for exploration, could be particularly valuable in adapting to such non-stationary environments.

Channel Estimation Overhead: Acquiring the CSI for the source-IRS and IRS-destination links is a significant challenge, especially for a large number of elements N^o. The overhead for this estimation must be accounted for in a complete system model.

Dynamic Environments: The proposed model assumes static channels. In reality, moving objects (people, vehicles) can cause rapid channel variations, requiring robust and low-latency optimization algorithms to track these changes effectively.

4.2. Hardware Imperfections

Our model assumes ideal IRS elements with continuous phase shifts and perfect reflection efficiency ($\alpha = 1$). In practice, hardware is imperfect. Phase shifters are often quantized (e.g., 1–2 bits), leading to quantization errors that degrade beamforming gain. Additionally, amplitude variations, mutual coupling between adjacent elements, and non-linear power consumption of the phase-shifting circuitry (P_e) can impact overall system performance. The energy efficiency gains reported would need to be re-evaluated under these non-ideal conditions. Integrating these impairments into the optimization problem is a critical next step.

These imperfections prevent the ideal phase shift modeled in (3) and (7), leading to a performance gap between theory and practice.

4.3. Scalability and Network Integration

The presented model considers a single IRS aiding a single user, for 6G systems. For scalability to multi-IRS, multi-cell, and multiuser scenarios, it is paramount. Deploying multiple IRSs introduces challenges like inter-surface interference, collaborative beamforming, and a combinatorial increase in the optimization complexity. Our current DS-PSO framework, while effective, would need to be scaled using distributed or hierarchical optimization methods to manage this complexity. Furthermore, integrating IRS control within existing network protocols and standards (e.g., for handover, resource allocation) is an open systems-level challenge that must be addressed for seamless adoption.

4.4. Computational Complexity and Real-Time Operation

The DS-PSO algorithm, while powerful, introduces a computational overhead compared to analytical solutions. The feasibility of its real-time operation depends on the coherence time of the channel. For slow-fading environments, the optimization can be performed offline or at a slow refresh rate. For high-mobility scenarios, low-complexity deep learning-based approximations of the optimization process could be developed to ensure real-time responsiveness, a direction we are actively pursuing.

4.5. Environmental Obstacles and Deployment

The optimal placement of IRSs, as hinted at in our simulation setup (Figure 2), is critical. The presence of unpredictable obstacles can break the assumed Line-of-Sight (LOS) links to the IRS. Practical deployment requires careful site-specific planning and the use of multiple distributed IRSs to ensure robust coverage. Our model provides the performance upper bound; practical gains will depend on strategic deployment to maximize the probability of strong LOS components.

4.6. Practical Constraints on Optimal LOS Gains

As rightly highlighted, the core of our optimized model relies on achieving the improved LOS channel gains (β_{sr}^o and β_{rd}^o) defined in Equation (33). Several practical constraints can limit the realization of these gains:

Physical Placement and Obstructions: Achieving these optimal gains is predicated on an obstruction-free placement of the IRS with a clear view to both the source and destination. In realistic environments like urban canyons or dense

indoor settings, identifying such a perfect location is a significant challenge. The presence of buildings, vegetation, or even moving objects like vehicles can easily disrupt the assumed LOS paths, reverting the channel to a weaker NLOS state and drastically diminishing the IRS's benefit.

Site-Specific Planning: The practical achievement of β^o is not merely a matter of geometry but requires extensive, site-specific radio planning. Factors such as material reflectivity, incidence angles, and the dynamic introduction of new obstacles must be considered; this necessitates intelligent and potentially adaptive deployment strategies, moving beyond the static, ideal-location assumption of our model.

These constraints do not invalidate our findings but rather define the critical boundary conditions for achieving our predicted performance. They underscore that the theoretical gains represent an upper bound, and their practical realization is contingent upon overcoming these deployment challenges through joint optimization of IRS placement, robust beamforming, and dynamic channel acquisition.

Accordingly, we fully agree that these practical challenges are significant and form the basis of ongoing research in the IRS community. Our work provides a crucial first step by establishing a theoretically optimized performance target under controlled conditions. The significant gains demonstrated (e.g., 366 Mbit/Joule at 10 bit/s/Hz) justify further investigation into overcoming these practical hurdles. The next phase of our research will explicitly focus on incorporating robust optimization under imperfect CSI, hardware constraints, and multiuser scalability, building directly upon the strong foundation laid by this paper.

5. Conclusions and Future Work

5.1. Conclusions

This study employed artificial intelligence (AI) to investigate the critical challenge of enhancing energy efficiency (EE) in IRS-aided 6G networks under high data rate constraints. To address the non-convex optimization problem inherent in IRS phase-shift design, an artificial intelligence (AI) framework was central to our methodology. Specifically, a novel hybrid Dynamic and Static Particle Swarm Optimization (DS-PSO) algorithm was developed and employed to configure the IRS elements intelligently. The results, generated through this AI-driven approach, demonstrate that our optimized Intelligent Reflecting Surfaces (IRS) model significantly outperforms standard IRS and SISO systems, achieving up to 269% higher energy efficiency at a data rate of 10 bits/s/Hz. (IRS^o) surpasses Triple-IRS by 46.4%, demonstrating that optimization is superior to hardware redundancy. Also, (IRS^o) at ultra-low data rates ($\leqslant 0.01$), compared to IRS with PSO and IRS with GA, exhibits exceptional performance, indicating that hybrid optimization may be necessary for enhanced energy efficiency. Therefore, it proves more effective than multi-IRS configurations and other AI-based optimizers from recent literature. This model's exceptional performance at elevated data rates validates its capacity to enhance transmission efficacy in sixth-generation (6G) communication networks.

5.2. Future Work

Future work will involve validating the findings using measured channel data from real-world scenarios and testing the algorithm's performance in more complex environments, such as urban canyons with strong non-line-of-sight (NLOS) components and interference.

The promising results of our model of (DS-PSO-IRS^o) establishes a strong foundation for several critical research avenues. Our immediate future work will focus on transitioning from theoretical models to robust, practical implementations for 6G systems, with efforts organized along four primary directions.

First, we will extend our model to dynamic and complex environments by replacing deterministic channels with sophisticated stochastic models that incorporate time-varying fading, shadowing, and random blockages. To manage this increased complexity and enable real-time adaptation, we will investigate advanced Deep Reinforcement Learning (DRL) algorithms. These agents will be designed to continuously learn and optimize IRS configurations amidst unpredictable interference and user mobility.

Second, we will explore the scalable integration of multiple IRSs within heterogeneous networks. This research will include studying collaborative beamforming between surfaces to create network-wide "smart radio environments" and managing inter-IRS interference. Furthermore, we will investigate the synergy between IRSs and Mobile Edge Computing (MEC), where IRSs can create favorable links for computational offloading to enhance communication and computational energy efficiency jointly.

Third, to bridge the simulation-to-reality gap, we will address practical hardware limitations and initiate experimental validation; this will involve developing strategies to compensate for phase quantization errors and amplitude losses in metasurfaces. The ultimate goal is to design a prototype and conduct field trials in a controlled testbed to validate the projected energy efficiency and data rate gains under real-world conditions.

Finally, a natural and critical extension of this work is its application to MIMO systems. The optimization problem in this context expands significantly to the joint optimization of active precoding/combining matrices at the transceivers and the passive phase shifts at the IRS, creating a coupled, high-dimensional non-convex problem. We will investigate modifying the DS-PSO algorithm to encode a larger solution vector encompassing all optimization variables, leveraging its explorative capabilities to maximize the overall spectral or energy efficiency of the MIMO-IRS system. Concurrently, we will explore the application of more complex AI architectures, particularly DRL, to manage this joint active and passive beamforming optimization with lower latency, assessing its practical robustness against measured channel data from real-world scenarios.

List of Abbreviations

AI	Artificial Intelligence
CSI	Channel State Information
DS-PSO	Dynamic and Static Particle Swarm Optimization
EE	Energy Efficiency
IRS	Intelligent Reflecting Surface
LOS	Line of Sight
MIMO	Multiple-Input Multiple-Output
NLOS	Non-Line-of-Sight
PSO	Particle Swarm Optimization
RIS	Reconfigurable Intelligent Surface
SE	Spectral Efficiency
SISO	Single-Input Single-Output
SNR	Signal-to-Noise Ratio
UMi	Urban Micro (cell)
6G	Sixth-Generation

Author Contributions

Conceptualization, methodology, software: J.K.S.A.-S.; validation, formal analysis: A.T.R.A.; investigation, resources, data curation, design and creation of figures, writing—original draft preparation, writing—review and editing, visualization, supervision, project administration: J.K.S.A.-S. and A.T.R.A. All authors have read and agreed to the published version of the manuscript.

Availability of Data and Materials

The content here.

Consent for Publication

The content here.

Conflicts of Interest

The authors declare no conflicts of interest regarding this manuscript.

Data Availability Statement

The data supporting the results of this study are available upon request from the corresponding author.

Funding

No external funding was received for this research.

Acknowledgement

The authors would like to thank and acknowledge the use of MATLAB and Microsoft Office for simulations, figures, tables, and full text preparation.

References

[1] X. Wang, J. Li, J. Wu, L. Guo, and Z. Ning, "Energy Efficiency Optimization of IRS and UAV-Assisted Wireless Powered Edge Networks," *IEEE J. Sel. Topics Signal Process.*, vol. 18, no. 7, pp. 1297–1310, 2024. doi: 10.1109/jstsp.2024.3452501.

[2] J. Li, Y. Huang, J. Wu, X. Wang, and Z. Ning, "Energy Efficiency Maximization for STAR-RIS and UAV-Assisted IUA: A Multi-Agent DRL Approach," *IEEE Internet Things J.*, vol. 12, no. 21, pp. 43936–43948, 2024. doi: 10.1109/jiot.2024.3518081.

[3] J. Wang and S. Chen, "Deep Reinforcement Learning-Based Secrecy Rate Optimization for Simultaneously Transmitting and Reflecting Reconfigurable Intelligent Surface-Assisted Unmanned Aerial Vehicle-Integrated Sensing and Communication Systems," *Sensors*, vol. 25, no. 5, p. 1541, 2025. doi: 10.3390/s25051541.

[4] P. Vishwakarma, S. N. Sur, S. Dhar, and D. Bhattacharjee, "IRS-Assisted SWIPT: Power Optimization Strategies for Green Communications," presented at the 2025 17th International Conference on COMmunication Systems and NETworks (COMSNETS), Bengaluru, India, Jan. 6–10, 2025, pp. 356–364

[5] H. Sadia, H. Iqbal, and S. Qadir, "Physical Layer Security in Intelligent Reflecting Surface-Enabled Small NOMA IoT Network," presented at the 2024 11th International Conference on Wireless Networks and Mobile Communications (WINCOM), Leeds, UK, July. 23–25, 2024, pp. 1–6.

[6] Q. Wu, T. Lin, X. Yu, Y. Zhu, and R. Schober, "Beamforming for PIN Diode-Based IRS-Assisted Systems Under a Phase Shift-Dependent Power Consumption Model," *IEEE Trans. Commun.*, vol. 73, no. 9, pp. 8092–8109, 2025. doi: 10.1109/tcomm.2025.3543228.

[7] W. Fang, W. Chen, Q. Wu, X. Zhu, Q. Wu, and N. Cheng, "Channel Characterization of IRS-Assisted Resonant Beam Communication Systems," *IEEE Trans. Commun.*, vol. 73, no. 9, pp. 7381–7397, 2025. doi: 10.1109/tcomm.2025.3550710.

[8] P. Siddhartha, L. Yashvanth, and C. R. Murthy, "Exploiting Beam-Split in IRS-Aided Systems via OFDMA," presented at the ICASSP 2025-2025 IEEE International Conference on Acoustics, Speech and Signal Processing (ICASSP), Hyderabad, India, Apr. 6–11, 2025, pp. 1–5.

[9] Y. Chen, Q. Wu, G. Chen, and W. Chen, "Spatial Multiplexing Oriented Channel Reconfiguration in Multi-IRS Aided MIMO Systems," *IEEE Trans. Veh. Technol.*, vol. 74, no. 6, pp. 9840–9845, 2025. doi: 10.1109/tvt.2025.3540067.

[10] M. Maashi et al., "Energy Efficiency Optimization for 6G Multi-IRS Multi-Cell NOMA Vehicle-to-Infrastructure Communication Networks," *Comput. Commun.*, vol. 225, pp. 350–360, 2024. doi: 10.1016/j.comcom.2024.07.018.

[11] J. Zhao, Q. Zhang, T. Ai, X. Wei, and F. Peng, "Optimal Reconfigurable Intelligent Surface Deployment for Secure Communication in Cell-Free Massive Multiple-Input Multiple-Output Systems with Coverage Area," *Electronics*, vol. 14, no. 2, p. 241, 2025. doi: 10.3390/electronics14020241.

[12] H. Nguyen-Thi, T. Kieu-Xuan, T. Le-Nhat, and A. Le-Thi, "Improving Energy Efficiency for Intelligent Reflecting Surface Assisted PD-NOMA in EH Relaying Network," *J. Inf. Telecommun.*, pp. 1–24, 2025. doi: 10.1080/24751839.2025.2464264.

[13] M. A. Ahmed, A. Baz, and M. M. Fouda, "Polyhedron Optimization for Power Allocation of Cell-Free Based IRS System," *IEEE Access*, vol. 12, pp. 76065–76073, 2024. doi: 10.1109/access.2024.3406479.

[14] A. Khaled, A. S. Alwakeel, A. M. Shaheen, M. M. Fouda, and M. I. Ismail, "Placement Optimization and Power Management in a Multiuser Wireless Communication System with Reconfigurable Intelligent Surfaces," *IEEE Open J. Commun. Soc.*, vol. 5, pp. 4186–4206, 2024. doi: 10.1109/ojcoms.2024.3426495.

[15] K. Wang, P. Liu, K. Liu, L. Chen, H. Shin, and T. Q. S. Quek, "Joint Beamforming and Phase-Shifting Design for Energy Efficiency in RIS-Assisted MISO Communication with Statistical CSI," *Phys. Commun.*, vol. 59, p. 102080, 2023. doi: 10.1016/j.phycom.2023.102080.

[16] H. Hashida, Y. Kawamoto, and N. Kato, "Mathematical Modeling and Deployment Optimization: Intelligent Reflecting Surface-Aided Communications Under Partial Blockages," *IEEE Trans. Cogn. Commun. Netw.*, vol. 11, no. 5, pp. 3306–3316, 2025. doi: 10.1109/tccn.2025.3534142.

[17] G. D. Verma, A. Mathur, Y. Ai, and M. Cheffena, "Mixed Dual-Hop IRS-Assisted FSO-RF Communication System with H-ARQ Protocols," *IEEE Commun. Lett.*, vol. 26, no. 2, pp. 384–388, 2021. doi: 10.1109/LCOMM.2021.3133202.

[18] A. Sikri, A. Mathur, and G. Kaddoum, "Joint Impact of Phase Error, Transceiver Hardware Impairments, and Mobile Interferers on RIS-Aided Wireless System Over κ-μ Fading Channels," *IEEE Commun. Lett.*, vol. 26, no. 10, pp. 2312–2316, 2022. doi: 10.1109/LCOMM.2022.3196756.

[19] C. Lai and R. Zhao, "An Autocorrelation-Based r-Stability Condition With Application in the Design of IIR Filters," *IEEE Signal Process. Lett.*, vol. 31, pp. 1389–1393, 2024. doi: 10.1109/lsp.2024.3396391.

[20] J. Li, J. Liu, and J. Wang, "Optimizing Spectrum and Energy Efficiency in IRS-Enabled UAV-Ground Communications," *Comput. Netw.*, vol. 256, p. 110911, Jan. 2025. doi: 10.1016/j.comnet.2024.110911.

[21] A. T. Alsahlanee, "Convergence Rate For Low-Pass Infinite Impulse Response Digital Filter," *J. Phys., Conf. Ser.*, vol. 1963, no. 1, p. 012103, Jul. 2021. doi: 10.1088/1742-6596/1963/1/012103.

[22] A. T. R. Alsahlanee and J. K. S. Al-Safi, "Improving Channel Gain of 6G Communications Systems Supported by Intelligent Reflective Surface," *Indones. J. Elect. Eng. Inform. (IJEEI)*, vol. 13, no. 1, pp. 57–68, Feb. 2025. doi: 10.52549/ijeei.v13i1.xxxx.

[23] J. Singh, N. A. Shelke, D. S. Hasan, M. Sajid, A. T. R. Alsahlanee, and K. Upreti, "Enhanced Learning in IoT-Based Intelligent Plant Irrigation System for Optimal Growth and Water Management," presented at the International Conference on Intelligent Systems Design and Applications, Olten, Switzerland, Dec. 11–13, 2023, pp. 231–240.

[24] J. K. S. Al-Safi and C. Kaleli, "A Correlation and Slope-Based Neighbor Selection Model for Recommender Systems," presented at the Next Generation of Internet of Things: Proceedings of ICNGIoT 2021, 2021, pp. 243–268.

[25] J. Al-Safi and C. Kaleli, "Item Genre-Based Users Similarity Measure for Recommender Systems," *Appl. Sci.*, vol. 11, no. 13, p. 6108, 2021. doi: 10.3390/app11136108.

[26] P. K. Keer, J. K. S. Al-Safi, S. B. G. T. Babu, and G. Ramesh, "Artificial Intelligence in Computer Network Technology in The Big Data Era," presented at the 2022 5th International Conference on Contemporary Computing and Informatics (IC3I), Uttar Pradesh, India, Dec. 14–16, 2022, pp. 2131–2135.

[27] E. Björnson, Ö. Özdogan, and E. G. Larsson, "Intelligent Reflecting Surface Versus Decode-and-Forward: How Large Surfaces Are Needed to Beat Relaying?," *IEEE Wireless Commun. Lett.*, vol. 9, no. 2, pp. 244–248, 2019. doi: 10.1109/LWC.2019.2953246.

[28] Ö. Özdogan, E. Björnson, and E. G. Larsson, "Intelligent Reflecting Surfaces: Physics, Propagation, and Pathloss Modeling," *IEEE Wireless Commun. Lett.*, vol. 9, no. 5, pp. 581–585, 2019. doi: 10.1109/LWC.2019.2961670.

[29] Q. Wu and R. Zhang, "Intelligent Reflecting Surface Enhanced Wireless Network via Joint Active and Passive Beamforming," *IEEE Trans. Wireless Commun.*, vol. 18, no. 11, pp. 5394–5409, 2019. doi: 10.1109/TWC.2019.2936025.

[30] J. Wang, H. Yang, Z. Wang, and C. Li, "MDRD-Based Channel State Information Acquisition Scheme for Intelligent Reflecting Surface-Aided Wireless Communication Systems," *Phys. Commun.*, vol. 71, p. 102667, 2025. doi: 10.1016/j.phycom.2024.102667.

[31] Z.-Q. He and X. Yuan, "Cascaded Channel Estimation for Large Intelligent Metasurface Assisted Massive MIMO," *IEEE Wireless Commun. Lett.*, vol. 9, no. 2, pp. 210–214, 2019. doi: 10.1109/LWC.2019.2950029.

[32] D. Tyrovolas et al., "Energy-Aware Trajectory Optimization for UAV-Mounted RIS and Full-Duplex Relay," *IEEE Internet Things J.*, vol. 11, no. 3, pp. 24259–24272, 2024. doi: 10.1109/jiot.2024.3390767.

[33] C. Y. Goh, C. Y. Leow, and R. Nordin, "Energy Efficiency of Unmanned Aerial Vehicle with Reconfigurable Intelligent Surfaces: A Comparative Study," *Drones*, vol. 7, no. 2, pp. 1–17, 2023. doi: 10.3390/drones7020076.

[34] E. Björnson and L. Sanguinetti, "Demystifying the Power Scaling Law of Intelligent Reflecting Surfaces and Metasurfaces," presented at the 2019 IEEE 8th International Workshop on Computational Advances in Multi-Sensor Adaptive Processing (CAMSAP), Le Gosier, Guadeloupe, Dec. 15–18, 2019, pp. 549–553.

[35] D. Bratton and J. Kennedy, "Defining a Standard for Particle Swarm Optimization," presented at the 2007 IEEE Swarm Intelligence Symposium, SIS 2007, Honolulu, HI, USA, Apr. 1–5, 2007, pp. 120–127.

[36] J. Kennedy and R. Eberhart, "Particle Swarm Optimization," presented at the ICNN'95-International Conference on Neural Networks, Perth, WA, Australia, Nov. 27–Dec. 1995, vol. 4, pp. 1942–1948.

[37] D. Sanchez, "DS-PSO: Particle Swarm Optimization with Dynamic and Static Topologies," Bowdoin College,

Bowdoin Digital Commons, Honors Projects, 2017.
[38] 3GPP, "Further Advancements for E-UTRA Physical Layer Aspects (Release 9)," 3rd Generation Partnership Project (3GPP), Technical Report 36.814, 2010.
[39] S. Penchala, S. K. Bandari, V. V. Mani, and A. Drosopoulos, "Controlled Wireless Channel using Multi-Antenna Multi-IRS Assisted Communication System: A Comprehensive Performance Analysis," *IEEE Latin America Trans.*, vol. 23, no. 2, pp. 114–124, 2025. doi: 10.1109/tla.2025.10851399.
[40] H. Nguyen-Thi, T. Kieu-Xuan, T. Le-Nhat, and A. Le-Thi, "Improving Energy Efficiency for Intelligent Reflecting Surface Assisted PD-NOMA in EH Relaying Network," *J. Inf. Telecommun.*, pp. 1–24, 2025. doi: 10.1080/24751839.2025.2464264.